Molecular Crystals and Liquid Crystals
Publication details, including instructions for authors and subscription information:
http://www.tandfonline.com/loi/gmcl20

Nanoscale Topography and Magnetic Structure of Nanocrystallized Nickel Electrodeposits

Lény Nzoghé-Mendome [a], Affaf Aloufy [b] & Jean Ebothé [a]

[a] Laboratoire de Microscopies & d'Etude de Nanostructures, E.A. n° 3799, UFR Sciences Exactes, Université de Reims, B.P. 138, 21 rue Clément Ader, 51685 Reims cedex 02, France

[b] Alexandria University, NNREL Centre, Faculty of Engineering, Alexandria, Egypt

Available online: 14 Feb 2012

To cite this article: Lény Nzoghé-Mendome, Affaf Aloufy & Jean Ebothé (2012): Nanoscale Topography and Magnetic Structure of Nanocrystallized Nickel Electrodeposits, Molecular Crystals and Liquid Crystals, 555:1, 32-39

To link to this article: http://dx.doi.org/10.1080/15421406.2012.634359

Mol. Cryst. Liq. Cryst., Vol. 555: pp. 32–39, 2012

ISSN: 1542-1406 print/1563-5287 online
DOI: 10.1080/15421406.2012.634359

Taylor & Francis
Taylor & Francis Group

Nanoscale Topography and Magnetic Structure of Nanocrystallized Nickel Electrodeposits

LÉNY NZOGHÉ-MENDOME,[1] AFFAF ALOUFY,[2] AND JEAN EBOTHÉ[1,*]

[1]Laboratoire de Microscopies & d'Etude de Nanostructures, E.A. n° 3799, UFR Sciences Exactes, Université de Reims, B.P. 138, 21 rue Clément Ader, 51685 Reims cedex 02, France
[2]Alexandria University, NNREL Centre, Faculty of Engineering, Alexandria, Egypt

The microstructure and magnetic properties of nickel films thick of 100 till 1000 nm are here investigated. They are deposited on polycrystalline Cu substrate by cathodic voltammetry (CV) technique varying the scan rate in the interval $0.17 \leq r \leq 1.67$ mV/s. Thicker and rougher samples grow at lower r values while thinner and smoother ones are obtained at the higher r values. All the samples obtained exhibit a negative strain indicating a compressive stress that decreases with the film thickness increase. The magnetic reversal of the Ni films is ruled by the spin rotation mechanism associated with their low squarness of about 28%. The study of their ferromagnetic-topography dependence reveals that their magnetic domains always remain of the Néel type $(MD)_N$ in the investigated r values according to the model of Zhao et al. [J. Appl. Phys. ***89****, 1325(2001)]. The magnetic anisotropy of the Ni samples exhibit a out-of-plane component that becomes sensitively marked with the increase of the film thickness.*

1. Introduction

The reactivity of a ferromagnetic film under an applied magnetic field proceeds from local structures consisted of magnetic domains (*MD*) and domain walls (*DW*) whose configurations are closely linked to their magnetic anisotropy. Actually, Maze-like domain patterns of $La_{0.7}Sr_{0.3}MnO_3$ films for instance have been associated with their perpendicular magnetic anisotropy [1]. Similarly, the weak dense stripe domains of Fe_{78} Si_{10} B_{12} films were found as the origin of that material out-of-plane anisotropy [2]. In that framework, the material microstructure and topography, associated to nano-structured and nano-crystallised films, play an important role. The deviation of their properties from those of bulky materials still remains an open investigation field for which the role of the film deposition technique and the related applied conditions are essential. Observations of the interdependence between the microstructure, the topography and the magnetism of thin films is nowadays largely reported. However, most of them concerns ultra-thin films made of some monolayers (ML)

*Address correspondence to Jean Ebothé, Laboratoire de Microscopies & d'Etude de Nanostructures, E.A. n° 3799, UFR Sciences Exactes, Université de Reims, B.P. 138, 21 rue Clément Ader, 51685 Reims cedex 02, France. Tel.: (33) 3 26 05 19 01; Fax: (33) 3 26 05 19 00; E-mail: jean.ebothe@univ-reims.fr

or samples having thickness values of a few hundreds nanometers. They are usually prepared in high vacuum systems from costly physical methods as ion implantation, sputtering and metal evaporation [3,4]. A cheaper procedure as electrodeposition has numerous acting parameters that can be explored for improving the film quality. In the present work, the investigated nano-crystallized nickel films are deposited this way on copper (Cu) substrate using cathodic voltammetry (CV) technique widely described elsewhere [5]. The dependence of their ferromagnetism on microstructure aspects induced by the deposition scan rate (r) is here examined from sample thickness values of some hundreds nano-meters till about one micron. An experimental approach to the film topography-magnetism dependence based on the concept of relative characteristics is here proposed.

2. Experimental Details

Ni electrodeposits are prepared in a three-electrode cell system from a 1M Ni $(SO_4)_2$ aqueous electrolyte (pH = 3.5) made of a FLUKA product. A stationary copper working electrode or deposition substrate of 0.5 cm^2 area is used, a saturated calomel one (SCE) serving for potential reference. The nickel films are obtained by cathodic voltammetry with a radiometer PGP 201 potentiostat, the related (C-V) curves being drawn at different scan rates (r) ranged in the interval $0.17 \leq r \leq 1.67$ mV/s commonly considered as low speeds [5]. The film thickness is measured from a commercial STRATAGem (SAMx France) software associated with the x-ray microanalysis, the related spectra being collected at about 25 kV for 100 s, as described in References 6 and 7. The Ni samples structure is analysed from a BRUCKER D8 ADVANCED x-ray apparatus with a Cu Kα irradiation $\lambda = 1.540$ Å. Their global magnetic properties are examined in ambient temperature with a vibrating sample magnetometer (VSM) of LAKE SHORE COMPANY. The samples topography and magnetic images are directly obtained from a scanning probe microscope (SPM) Nanoscope IIIa (VEECO) operating in atomic force microscope (AFM)/magnetic force microscope (MFM) dual mode. Magnetic CoCr-coated tips of approximately 17 nm apex radius with a cantilever of 6 Nm^{-1} spring coefficient are used here with a resonance frequency of about 70 kHz. MFM analysis is performed in the tapping/lift mode, which allows the collection of both the topography and the magnetic-force images of the same sample surface area. The oscillating magnetic cantilever shift is measured at a constant tip-sample distance of about 100 nm with a spatial resolution of 10 nm. In all cases, the tip is initially magnetized with a field perpendicular to the sample plane, no external magnetic field being applied during the Ni sample analysis.

3. Results and Discussion

In the present work, (CV) scan rate is the main acting parameter of the film deposition process and hence the one at the origin of any change in the film microstructure including the surface morphology and thickness. These particular aspects of the Ni samples are analysed first as they can provide some interesting indications for the study of their global and local magnetic characteristic as proposed in the next sub-section.

3.1 Microstructure and Topography Evolution of Ni Electrodeposits

We showed previously that Ni electrodeposits formed on Cu substrate by our CV method in the present conditions always grow in a faced centred cubic (fcc) phase of [220] preferred orientation, regardless of the r value [5]. The 3D AFM images of Fig. 1 denotes that the

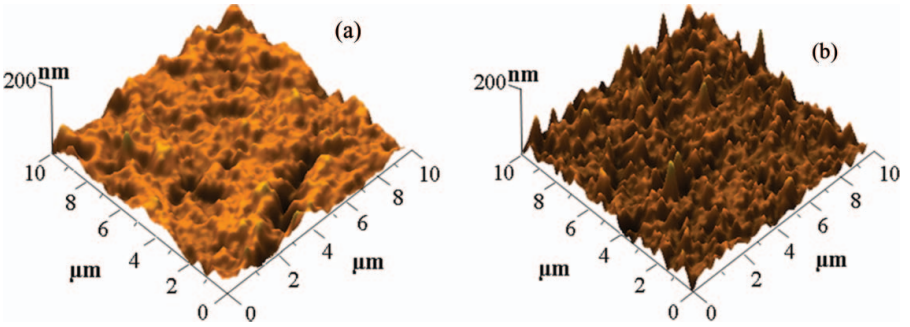

Figure 1. 3D AFM images of Ni electrodeposits obtained at two scan rate values: a) $r = 1.67$ mV/s ($d = 104$ nm); b) $r = 0.17$ mV/s ($d = 1000$ nm).

lower scan rate $r = 0.17$ mV/s engenders a marked granular feature of pretty needle-like particles as it appears in Fig. 1(b) while $r = 1.67$ mV/s leads to more rounded ones in Fig. 1(a). That denotes somehow a probable change in the film growth process induced by r. Evaluation of the grain lateral size or mean diameter (D) from the [220] X-ray main peak using the Debye-Scherrer formula, as developed elsewhere [8], concurs very well here with the values obtained by the fast Fourier transformer (FFT) calculation performed with the film AFM images. Figure 2 clearly depicts a decrease of both D and the film thickness (d) with the increase of r. This result indicates that low r values favour the grain formation and the global material deposition as a higher stabilization of Ni ad-atoms at the film-substrate interface is expected in that case due to a better charge transfer equilibrium. The results in Table 1 show that the lattice mismatch between Ni and Cu leads to a compressive stress effect during the film formation regardless of r value. Actually, the lattice parameter of the Ni samples deduced from x-ray analysis always remains lower than $a_0 = 3.5241$ Å of bulk. One observes that thinner Ni films with smaller grains are less stressed than thicker ones with bigger grains.

The topography modification of the Ni films due to scan rate is investigated using the Family-Viscek method widely described in our previous works [5,9]. The results proposed in Table 1 show that the measured saturated root-mean-square surface roughness (σ) of the film decreases with the increase of r. However, as the film thickness and surface roughness both are affected by the scan rate, only the relative roughness (σ/d) can quantitatively

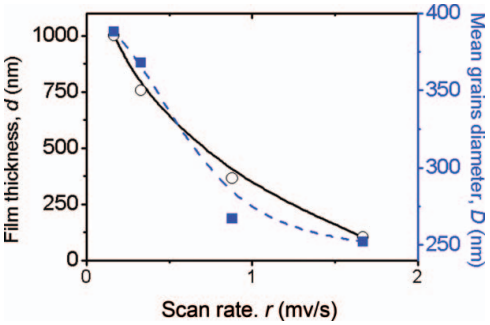

Figure 2. Role of the deposition scan rate on specific characteristics of Ni electrodeposits: a) – the film thickness (d); b) – the mean grain diameter (D).

Table 1. Topography and strain dependences of the Ni films on the deposition scan rate for the Ni/Cu system

Scan rate r (mV/s)	RMS surface roughness σ (nm)	Lattice parameter a (Å)	Strain ε (%)
0.17	91	3.5217	−0.07
0.33	95	3.5194	−0.13
0.88	33	3.5082	−0.45
1.67	28	3.5038	−0.58

describe the effective topography change. Fig. 3 shows that (σ/d) drastically increases with scan rate, particularly from $r \approx 0.88$ mV/s. The roughness-thickness dependence of the inset displays the strong surface perturbation of Ni films at the higher thickness range, the smoothness increasing with d value. This result is quite in agreement with those of most reports for which the increase of film thickness leads to the one of grain size and surface roughness [10].

3.2 Magnetic Characteristics of the Investigated Ni Electrodeposits

Scan rate is a deposition parameter that has no direct link with the material physical properties. However, its induced effect can be examined through the thickness or other microstructure characteristics of the related Ni films. The study of the hysteresis loop profile is the common approach to investigation of the sample global magnetic properties. For that purpose, two samples corresponding to the extreme r values have been analysed under a parallel applied field interval $-1.5 < H_{//} < +1.5$ KOe. The results of Fig. 4 shows that although the reported hysteresis loops have nearly the same shape, the sample thick of $d = 1000$ nm ($r = 0.17$ mV/s) gives rise to a more tilted profile than the thinnest sample of $d = 104$ nm ($r = 1.67$ mV/s). This implies some modification of the microscopic magnetic parameters of the films induced by r value that seems worthwhile to be examined within the investigated film thickness amplitude. The evolution of the samples coercivity (H_c)

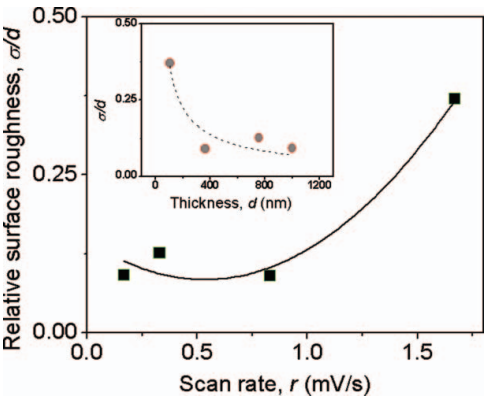

Figure 3. Effect of the deposition scan rate on the relative surface roughness of Ni films and (in the inset) the one of the film thickness on their relative surface roughness.

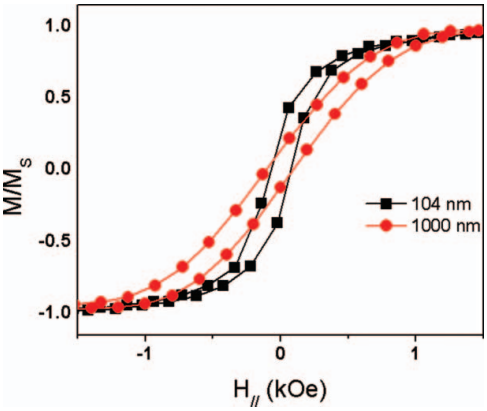

Figure 4. Magnetic hysteresis loops: of the 104 ($r = 1.67$ mV/s) and 1000 ($r = 0.17$ mV/s) nm-thick Ni samples under the parallel filed applied magnetic field.

and squareness $S = (M_r/M_s)$ defined as the ratio of the remanence (M_r) on the saturation magnetisation (M_s) as shown in Fig. 5 denotes the occurrence of some specific induced effects of the scan rate. It can be observed here that S is practically independent to the film thickness, its value being always located at $S \approx 0.28$. That low S value (≤ 0.5) indicates that the magnetic reversal of the films are here ruled by the spin rotation mechanism, regardless r value. Therefore, the coercitivity represents the necessary magnetic energy to overcome any hitch to that rotating mechanism. The reported evolution of the coercivity in Fig. 5 denotes that the proximity of Hc values obtained from the samples grown at the two extreme r values does not reflect the real scan rate induced effect. One sees that Hc value decreases with the increase of d till a critical value $d_c \approx 375$ nm corresponding to a minimal coercivity $(Hc)_m \approx 58$ Oe from which an increase of Hc appears for $d > d_c$. Owing to the fact that there is no structural and textural change in the films due to r, as mentioned above, the behaviour of Hc is likely to be explained by a competition between two listed factors. The decrease of Hc at the smaller d values is an agreement with the increase of the grain size with d showed in Fig. 2. This fact favours the growing of the magnetic domain (MD) and eases the spin rotation mechanism. As shown in Table 1, the film strains

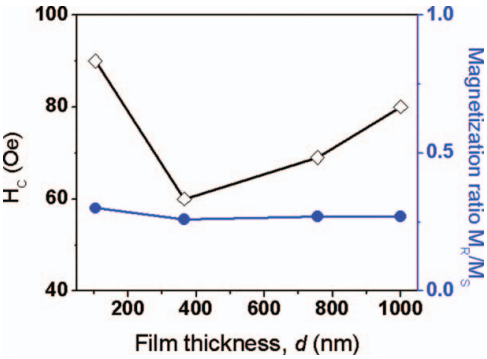

Figure 5. Dependence of the global magnetic characteristics of Ni electrodeposits on the sample thickness: a) squareness $S = (M_r/M_s)$; b) coercivity (H_c).

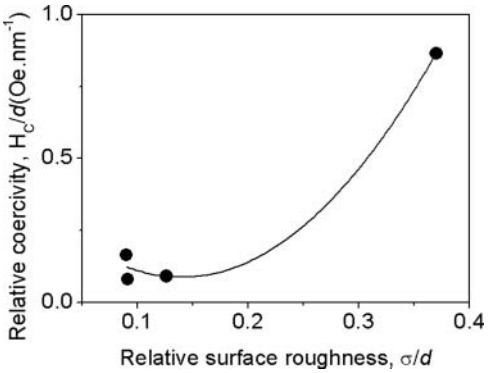

Figure 6. Dependence of coercivity on the surface roughness of the Ni electrodeposits in the relative approach of the film's properties.

in that d region are negligible ($\varepsilon < 0.15\%$). The increase of the film strain above d_c can thus explain the observed coercivity enhancement since the grain size D increase in that region is insignificant.

The direct examination of the topography effect on the film magnetic properties can be consistently undertaken only with samples having the same thickness. This requirement suggests the use of relative properties referring to the film unit thickness. This method is relevant here as the investigated Ni samples exhibit in Fig. 3 relatively large roughness amplitude. In that case, the obtained coercivity increase with the Ni film's roughness shown in Fig. 6 concurs quite well with the experimental results mostly based on hard etching treatments of some ferromagnetic film-substrate systems [11–13]. This change in the film coercivity goes together with a modification of the material *DW* thickness and *MD* size (w) as they are both also linked to the film thickness and roughness [14,15,16]. The statistical measurements of the Ni film's *MD* size from the MFM images as proposed by Hsieh et al. [16] and also Dumas-Bouchiat et al. [17] leads to assess the film roughness effect on the magnetic micro and nano-structures of the Ni electrodeposits. The results of Fig. 7 reveal that w always decreases with the increase of the relative roughness. This behaviour agrees

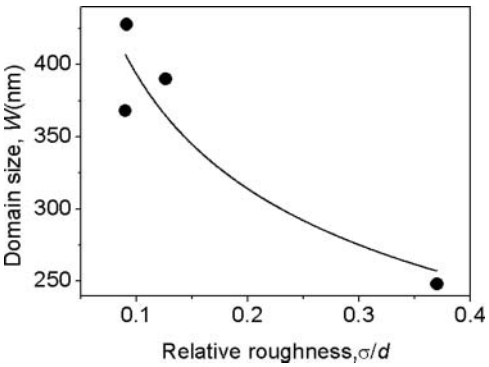

Figure 7. Dependence of the magnetic domain size on the relative surface roughness of the Ni electrodeposits.

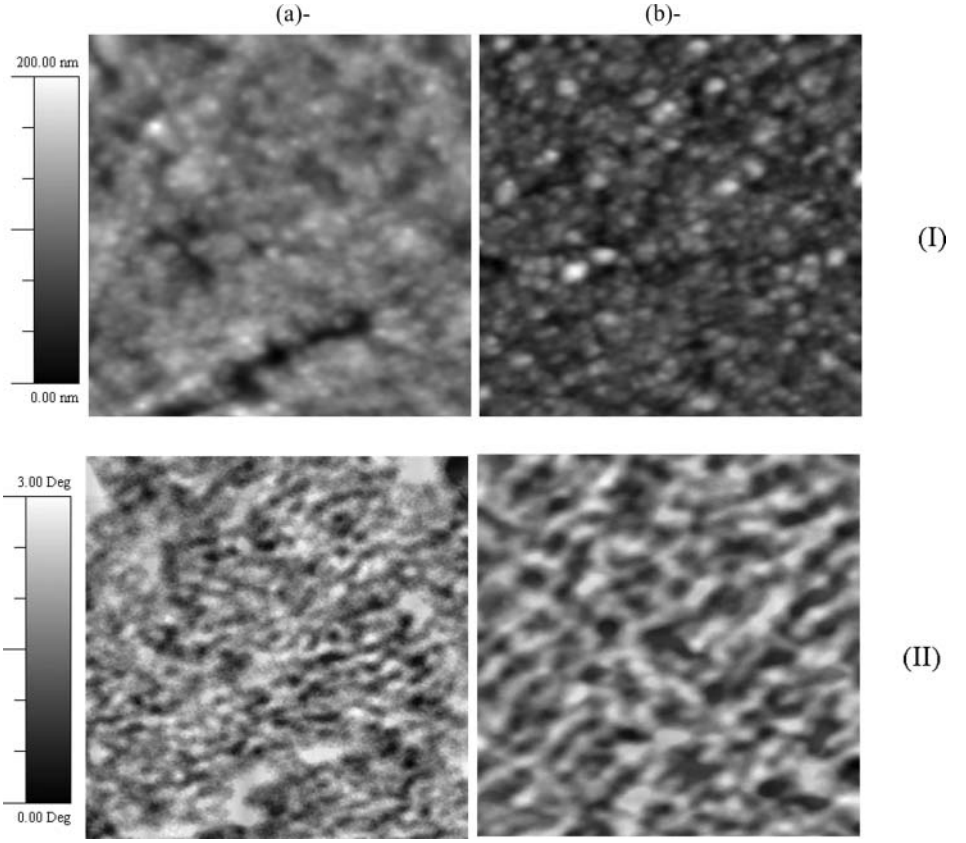

Figure 8. SPM images of the two extreme Ni electrodeposits obtained at : a) $r = 1.67$ mV/s ($d = 104$ nm) and; b) $r = 0.17$ mV/s ($d = 1000$ nm) with (**I**) the topography AFM images and (**II**) the MFM magnetic phase images.

quite well with the prediction of Zhao et al. [18] for which the decrease of w versus film roughness is characteristic of the Néel domains type $(MD)_N$.

In agreement with the results of Fig. 1, the 2D-AFM topography images (**I**) of Fig. 8 mainly depict the grain size difference of the Ni samples. However, they always remain the necessary reference for the study of their magnetic configuration (**II**) as the same surface area is concerned. For both of the considered samples, one sees that the granular features of the topography images of Figs. 8I are not systematically reproduced in the magnetic phases of Figs. 8II as recently reported elsewhere [19]. Obviously, the bright and dark dots of these MFM images respectively reflect the up (repulsive interaction) and down (attractive interaction) electron spin states. However, the topography of the thinnest sample ($d = 104$ nm) related to $r = 1.67$ mV/s as shown in Fig. 8I(a) already leads to a serpentine magnetic configuration of Fig. 8II(a). This magnetic configuration is more marked in Fig. 8II(b) with bigger *MD*s and *DW*s of the thicker film ($d = 1000$ nm) obtained $r = 0.17$ mV/s. Note that this particular change is in agreement with the increase of D depicted in Fig. 8I(a). It should be notice that the serpentine pattern is commonly associated with multi-domain magnetic features [15,17,20] associated with a presence of a out-of plane magnetic anisotropy in the material. The change induced by the scan rate parameter can thus be interpreted as an

increase of the perpendicular component of the film magnetic anisotropy occurred with the increase of the film thickness.

4. Conclusion

Although the (CV) method is currently used for getting information on the electrochemical processes involved at the film (working electrode)/deposition bath (electrolyte) interface, we showed in the present work that this method can successfully lead to the formation of nano-structured films. We here evidenced the crucial role of the scan rate on the topography and morphology of the Ni nano-structured electrodeposits. The relative wide amplitudes of the film thickness and roughness obtained permitted to reveal the ferromagnetism-microstructure and topography dependences using the relative approach to the Ni films properties without any additional surface treatment of the samples. The behaviour of their coercivity (H_c) and magnetic domain size (w) versus σ agrees quite well with the prediction of the topography based model of Zhao et al. [18]. The study of the MFM images reveal a serpentine magnetic feature regardless the film thickness or deposition scan rate used. However, the more neatly ripped magnetic feature obtained with the thicker film indicates the presence of a more marked out-of-plane magnetic anisotropy in that sample than in the thinner one.

References

[1] Dho, J., & Hur, N. H. (2007). *J. Magn. Magn. Mat.*, *318*, 23.
[2] Sun, Z. G., Kuramochi, H., & Akinaga, H. (2005). *Appl. Surf. Sci.*, *244*, 489.
[3] Kohler, M., Zweck, J., Bayreuther, G., Fisher, P., Schutz, G., Denbeaux, G., & Attwood, D. (2002). *J. Magn. Magn. Mat.*, *240*, 79.
[4] Ausanio, G., Iannotti, V., Lanotte, L., Carbucicchio, M., & Rateo, M. (2001). *J. Magn. Magn. Mat.*, *226-230*, 1740.
[5] Nzoghé-Mendome, L., Ebothé, J., Aloufy, A., & Kityk, I. V. (2008). *J. Alloys &Compounds*, *459*, 232.
[6] Pouchou, J.-L. (1993). *Anal. Chem. Acta*, *283*, 81.
[7] Benhayoune, H., Dumelié, N., & Balossier, G. (2005). *Thin Solid Films*, *493*, 113.
[8] Naccereddine, C., Layadi, A., Guittoum, A., Chérif, S-M., Chauveau, T., Billet, D., Ben Youssef, J., Bourzami, A., & Bourahli, M.-H. (2007). *Mater. Sci. Eng. B.*, *136*, 197.
[9] Hiane, M., & Ebothé, J. (2001). *Eur Phys. J. B.*, *22*, 485.
[10] Tang, Y., Zhao, D., Shen, D., Zhang, J., Li, B., Lu, Y., & Fan, X. (2008). *Thin Solid Films*, *516*, 2094.
[11] Malyuntin, V. I., Osukhovski, V. E., Vorobiev, Yu. D., Shishkov, A. G., & Yudin, V. V. (1981). *Phys. Status Solidi A*, *65*, 45
[12] Li, M., Wang, G.-C., & Min, H.-G. (1998). *J. Appl. Phys.*, *83*, 5313.
[13] Li, M., Zhao, Y.-P., Wang, G.-C., & Min H.-G. (1998). *J. Appl. Phys.*, *83*, 6287.
[14] Chioncel, M. F., Nagaraja, H. S., Rossignol, F., & Haycock, P. W. (2007). *J. Magn. Magn. Mat.*, *313*, 135.
[15] Hameed, S., Talagala, P., Naik, R., Wenger, L. E., Naik, V. M., & Proksch, R. (2001). *Phys. Rev. B.*, *64*, 184406.
[16] Hsieh, C. T., Liu, J. Q., & Lue, J. T. (2005). *Appl. Surf. Sci.*, *252*, 1899.
[17] Dumas-Bouchiat, F., Nagaraja, H. S., Rossignol, F., Champeaux, C., & Catherinot, A. (2005). *Appl. Surf. Sci., 247*, 76
[18] Zhao, Y.-P., Gamache, R. M., Wang, G-C., Lu, T-M., Palansantzas, G., & De Hosson, J. Th. M. (2001). *J. Appl. Phys.*, *89*, 1325.
[19] Nzoghé-Mendome, L., Ebothé, J., & Molinari, M. (2011). *J. Appl. Phys.*, *109*, 024904.
[20] Coïsson, M., Vinai, F., Tiberto, P., & Celegatto, F. (2009). *J. Magn. Magn. Mat.*, *321*, 806.